

**qPlus atomic force microscopy of the Si(100) surface: Buckled, split-off, and added dimers**

A. Sweetman, S. Gangopadhyay, R. Danza, N. Berdunov, and P. Moriarty

Citation: [Applied Physics Letters](#) **95**, 063112 (2009); doi: 10.1063/1.3197595

View online: <http://dx.doi.org/10.1063/1.3197595>

View Table of Contents: <http://scitation.aip.org/content/aip/journal/apl/95/6?ver=pdfcov>

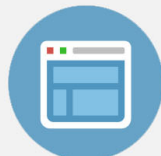
Published by the [AIP Publishing](#)

---



## Re-register for Table of Content Alerts

Create a profile.



Sign up today!



## qPlus atomic force microscopy of the Si(100) surface: Buckled, split-off, and added dimers

A. Sweetman, S. Gangopadhyay, R. Danza, N. Berdunov, and P. Moriarty<sup>a)</sup>  
*The School of Physics and Astronomy, The University of Nottingham, Nottingham NG7 2RD,  
 United Kingdom*

(Received 15 May 2009; accepted 10 July 2009; published online 14 August 2009)

Dimer configurations at the Si(100) surface have been studied with noncontact atomic force microscopy in the qPlus mode at 77 K, using both large (10 nm peak to peak) and small (0.5 nm peak to peak) oscillation amplitudes. In addition to the  $p(2 \times 1)$ ,  $p(2 \times 2)$ , and  $c(4 \times 2)$  reconstructions of the pristine surface, a variety of defect types including ad-dimers, vacancies, and split-off dimers have been imaged. Our data appear at odds with the currently accepted structural model for split-off dimers. At low oscillation amplitudes the degree of apparent dimer buckling can be “tuned” by varying the frequency shift set point. © 2009 American Institute of Physics. [DOI: 10.1063/1.3197595]

The Si(100) surface is a fascinating example of the rich physics that can arise from a relatively simple system. Although it has been understood for quite some time that the basic building block of each of the clean surface phases is the silicon dimer,<sup>1–4</sup> the origin and dynamics of the  $p(2 \times 2)$  and  $c(4 \times 2)$  reconstructions have been the subject of a remarkable amount of debate.<sup>5–7</sup> At the center of this debate has been the issue of dimer buckling and the associated energy barrier associated with flipping between two buckled states.

The small energy barrier ( $\sim 100$  meV)<sup>4,8</sup> associated with dimer flipping means that “noninvasive” imaging of the ground state of the Si(100) surface presents a particular challenge for scanning probe microscopy. The probe can have a very strong influence on the Si(100) surface structure and, indeed, the surface phase observed depends on the strength of the tip-sample interaction.<sup>6,7,9,10</sup> It is therefore natural to investigate the surface with the most sensitive scanning probe method available, namely qPlus noncontact atomic force microscopy (NC-AFM).<sup>11</sup> In this configuration a quartz tuning fork is used instead of a silicon cantilever and the greatly increased stiffness allows subnanometer to subangstrom oscillation amplitudes to be used. To that end we present here results from an investigation of the Si(100) surface using the qPlus technique. (Previous NC-AFM imaging of the Si(100)-(2 × 1) surface using low oscillation amplitudes involved off-resonance excitation and STM-based feedback<sup>12</sup>).

We used heavily boron-doped (1 mΩ cm) Si(100) for all of the qPlus experiments described here. The Si(100) samples (3 × 10 mm<sup>2</sup>) were first degassed at 600 °C for three to four hours in UHV before being flash annealed to approximately 1200 °C (for 10–30 s) while the pressure was kept below 5 × 10<sup>-10</sup> mbar, rapidly cooled to 900 °C, and then slowly cooled ( $\sim 3$  °C/s) to room temperature. The sample was then transferred to a commercial low temperature (LT) scanning tunneling microscopy (STM)-qPlus AFM instrument (Omicron Nanotechnology GmbH) cooled to 77 K. We used qPlus sensors (Omicron) comprising an etched

W tip glued to a tine of the quartz tuning fork. The sensors were transferred to the LT STM-AFM with no prior cleaning treatment (such as e-beam annealing or ion sputtering). Instead, we relied on bias voltage pulsing during STM scanning to obtain atomic resolution. Typically, we found it took on average four to six hours of scanning and pulsing (up to  $\pm 10$  V pulses were applied) to obtain high quality atomic resolution STM images with qPlus tips. It is therefore possible that the tips we use for qPlus imaging are silicon, rather than tungsten, terminated.

The resonant frequency and quality factor of the sensor with the W tip attached—as measured by impulse excitation of the tuning fork with subsequent Fourier transformation of the response—were between 20 and 25 kHz and 5000–15 000, respectively, (at 77 K). The tuning fork was mechanically oscillated and scanned in constant frequency shift mode. Damping and tunnel current signals were recorded simultaneously with the topography. Measurements of the frequency shift,  $df$ , versus tip bias,  $V$ , were used to determine the effective contact potential. This was generally in the 100 to 800 meV range, although in a small number of cases the minimum of the  $|df|$  versus  $V$  curve was at 0 V. The tuning fork oscillation amplitude was calibrated using both a measurement of the onset of the tunnel current signal as the sensor driving signal was increased and via the constant normalized frequency shift method introduced by Giessibl.<sup>11</sup> Both methods gave identical results within experimental error.

Figure 1(a) is a qPlus image of the Si(100) surface taken at large oscillation amplitude (10 nm peak to peak) with a  $df$  setpoint of  $-4.9$  Hz and an applied sample bias of +0.1 V. A  $p(2 \times 1)$  arrangement of symmetric surface dimers is observed. Although the  $p(2 \times 2)$  and  $c(4 \times 2)$  phases were occasionally observed using large amplitudes (data not shown here), in general, the data were of poor quality and overwhelmingly we found that, for large (approximately few nanometers) amplitude probe oscillations, successful atomic resolution imaging showed  $p(2 \times 1)$  symmetry. As was also found in recent high amplitude NC-AFM studies of the Si(100)-(2 × 1) surface using silicon cantilevers,<sup>13</sup> the separation of the maxima comprising each dimer feature in Fig. 1(a) is 2.9 Å ( $\pm 0.2$  Å). Figure 1(a) also shows images of two

<sup>a)</sup>Electronic mail: philip.moriarty@nottingham.ac.uk.

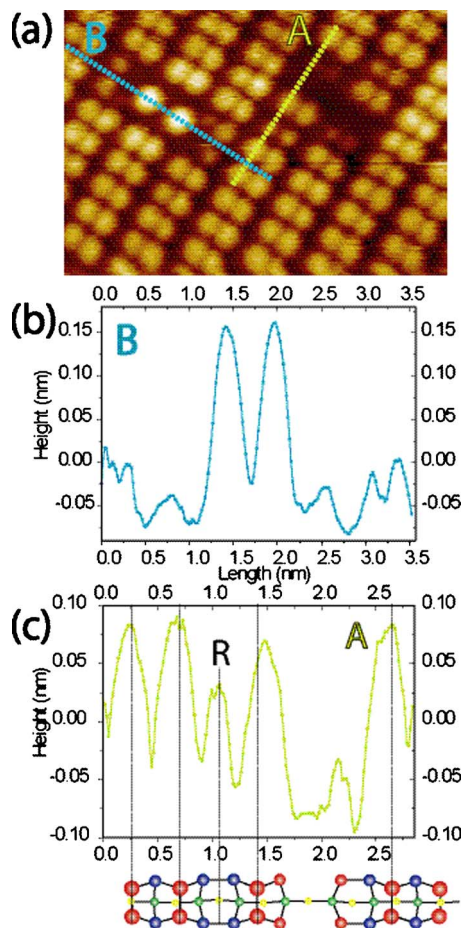


FIG. 1. (Color online) (a) NC-AFM image taken using a qPlus sensor ( $5.42 \times 3.75 \text{ nm}^2$ ) of the Si(100) surface taken at 77 K with an oscillation amplitude of 10 nm peak to peak,  $df = -4.9 \text{ Hz}$ , and  $V_{\text{sample}} = +0.1 \text{ V}$ . In addition to the  $p(2 \times 1)$  surface reconstruction, two surface defects are observed: a boron-induced ad-dimer (labeled B) and a 1+2-DV defect cluster; (b) Line profile through the ad-dimer defect; (c) Line-profile through 1+2-DV defect cluster and comparison with currently accepted structural model (Ref. 17). R represents the position of the recessed dimer observed in our images.

of the primary types of defect which occur at the Si(100) surface: A boron-induced ad-dimer (labeled B) and 1+2 dimer vacancy (1+2-DV) defect clusters.

Line profiles through the boron-induced and 1+2-DV defects are shown in Figs. 1(b) and 1(c) respectively. Focusing on the boron-induced structure first, we note that there is a strong qualitative similarity between our qPlus AFM images of this defect and the STM data of Liu *et al.*<sup>14</sup> taken at relatively high ( $> +2.0 \text{ V}$ ) bias voltages. Our qPlus data are, overall, in much better agreement with the silicon ad-dimer model put forward by Liu *et al.* than with previously proposed structures.<sup>15,16</sup>

In Fig. 1(c), we compare a line profile through a qPlus image of a 1+2-DV cluster to the currently accepted structural model for this type of defect, proposed by Wang, Arias, and Joannopoulos.<sup>17</sup> The 1+2-DV defect has been studied in some detail using STM by a number of groups including, most recently and most comprehensively, Schofield *et al.*<sup>18</sup> Although our qPlus AFM data are in broad agreement with the primary structural features of the 1+2-DV defect, there is a clear discrepancy with regard to the rebonding of atoms expected at the position marked “R” in Fig. 1(c). At position R, instead of an absence of intensity due to the rebonding

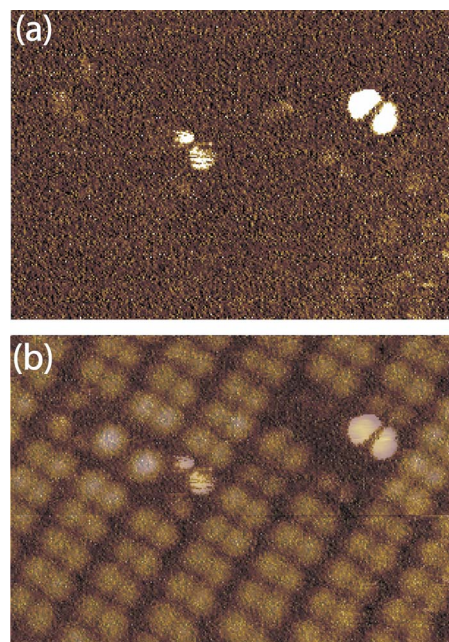


FIG. 2. (Color online) (a) Tunnel current image acquired in parallel with the qPlus NC-AFM image shown in Fig. 1(a). The tunnel current scale ranges from 0 to 2.8 pA. (b) Overlay of Fig. 1(a) and (a).

(and lack of dangling bonds) associated with the vacancy, we observe a dimerlike surface feature at an apparent height of approximately  $0.5 \text{ \AA}$  below the dimers of the surrounding ( $2 \times 1$ ) reconstructed area. Prior to the proposal of Wang *et al.* of the rebonded 1+2-DV structure, Ihara *et al.*<sup>19</sup> put forward an interstitial dimer model involving a dimer which is recessed into the surface. Although the *ab initio* calculations of Wang *et al.* ruled out the interstitial dimer model, we note that a recessed dimer of this type is compatible with the R feature we observe.

An important advantage of the qPlus technique, as compared to conventional NC-AFM, is the relative ease with which tunnel current images can be acquired in parallel with the frequency shift data. Given that a voltage of  $+0.1 \text{ V}$  was applied during the acquisition of Fig. 1(a), the tunnel current signal acquired in parallel [Fig. 2(a)] is sensitive to near-Fermi level empty states. While the lack of tunnel current associated with the boron-induced ad-dimer is not at all unexpected on the basis of the experimental and simulated STM data of Liu *et al.*,<sup>14</sup> the observation of current maxima located above the 1+2 DV feature is surprising. In Fig. 2(b), we have overlaid the tunnel current image on the qPlus topography to illustrate that the tunnel current maxima are located directly above the split-off dimer feature.

Hamers and Köhler<sup>20</sup> and Ukraintsev *et al.*<sup>21</sup> found that only so-called C-type defects were associated with a high density of states at the Fermi level and that, for single and double vacancies, there was little or no state density at voltages less than 200 meV. What is intriguing about the image in Fig. 2(a) [and the overlay in Fig. 2(b)] is that while one of the 1+2 DV defects is associated with a very distinct tunnel current “signature,” a neighboring split-off dimer, in apparently the same bonding geometry, exhibits no such strong maximum in the tunnel current image. One possibility is that the difference in the electronic character of the defect clusters is due to subsurface boron (or another impurity). In addition, Brown *et al.*<sup>22</sup> have highlighted the importance of



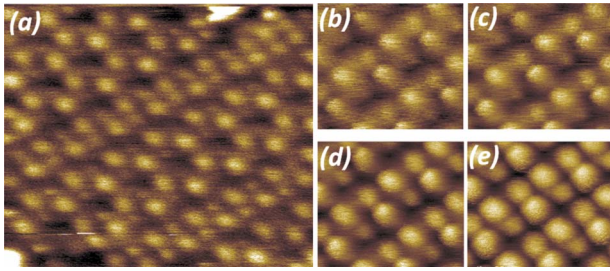


FIG. 3. (Color online) (a) qPlus AFM image of the Si(100) surface taken at 77 K with a peak to peak oscillation amplitude of 0.7 nm, a sample bias of +0.3 V, and  $df = -10.9$  Hz; (b)–(e) Effect of changing the setpoint  $df$  on the resolution of the lower atom of each buckled dimer;  $df = -26.1$  Hz,  $-27$  Hz,  $-28$  Hz, and  $-30$  Hz for images (b)–(e), respectively. [For (b)–(e) the oscillation amplitude and sample bias are 0.5 nm peak to peak and +0.8 V, respectively].

band-bending effects in the imaging of defects on Si(100)-(2 × 1). It is clear that a systematic qPlus AFM-STM study of defects at the Si(100) surface, combined with density functional theory (DFT) calculations (including the role of the tip-sample interaction), is required and, indeed, an investigation of this type is underway in our laboratory.

With lower, subnanometer, sensor oscillation amplitudes,  $c(4 \times 2)$  and  $p(2 \times 2)$  reconstructions are routinely observed [Fig. 3(a)]. An important aspect of Fig. 3(a), however, is that the “visibility” of the lower atom of each of the buckled dimers in the  $c(4 \times 2)$  and  $p(2 \times 2)$  phases varies strongly across the image. In Figs. 3(b)–3(e) we show the influence of changing the  $df$  setpoint (from  $-26$  to  $-30$  Hz) on the qPlus image. It is clear that although there is a gradual improvement in the resolution of the lower atom of each buckled dimer with a concomitant “evolution” of the apparent surface reconstruction toward a more symmetric [ $p(2 \times 1)$ ] structure, there is a great deal of residual asymmetry in Fig. 3(e). This residual asymmetry was predicted in DFT calculations<sup>7</sup> and arises from the dynamics of the tip-sample interaction at 77 K. A key goal of future work is to determine, using  $df$  versus  $z$  spectroscopy at 4 K, the force required to flip the dimer configuration between two buckled states.

In conclusion, we have imaged a variety of dimer configurations at the Si(100) surface using the qPlus NC-AFM technique. Our qPlus data are in good agreement with the model very recently put forward by Liu *et al.*<sup>14</sup> for the B-induced ad-dimer defect but are at odds with the currently

accepted model of the 1+2-DV cluster. We show that the apparent degree of dimer buckling depends sensitively on the setpoint  $df$  value.

The work described in this paper was funded by the U.K. Engineering and Physical Sciences Research Council (EPSRC) under Grant Nos. EP/G007837/1 and EP/C534158/1 and by the European Commission networks Grant Nos. MEST-CT-2004-506854 (NANOCAGE) and MRTN-CT-2004-005728 (PATTERNS). We gratefully acknowledge the advice and help of Juergen Koeble, Omicron Nanotechnology, in relation to the qPlus instrument. We also thank Peter Beton (Nottingham), John Boland, and Boris Naydenov (Trinity College Dublin) for helpful discussion.

<sup>1</sup>D. J. Chadi, *Phys. Rev. Lett.* **43**, 43 (1979).

<sup>2</sup>P. Krüger and J. Pollmann, *Phys. Rev. Lett.* **74**, 1155 (1995).

<sup>3</sup>R. M. Tromp, R. J. Hamers, and J. E. Demuth, *Phys. Rev. Lett.* **55**, 1303 (1985).

<sup>4</sup>R. A. Wolkow, *Phys. Rev. Lett.* **68**, 2636 (1992).

<sup>5</sup>For reviews, see T. Uda, H. Shigekawa, Y. Sugawara, S. Mizuno, H. Tochiyama, Y. Yamashita, J. Yoshinobu, K. Nakatsuji, H. Kawai, and F. Komori, *Prog. Surf. Sci.* **76**, 147 (2004); J. Yoshinobu, *Prog. Surf. Sci.* **77**, 37 (2004).

<sup>6</sup>Y. J. Li, H. Nomura, N. Ozaki, Y. Naitoh, M. Kageshima, Y. Sugawara, C. Hobbs, and L. Kantorovich, *Phys. Rev. Lett.* **96**, 106104 (2006).

<sup>7</sup>L. Kantorovich and C. Hobbs, *Phys. Rev. B* **73**, 245420 (2006).

<sup>8</sup>K. Hata, Y. Sainoo, and H. Shigekawa, *Phys. Rev. Lett.* **86**, 3084 (2001).

<sup>9</sup>K. Sagisaka, D. Fujita, and G. Kido, *Phys. Rev. Lett.* **91**, 146103 (2003).

<sup>10</sup>K. Sagisaka and D. Fujita, *Phys. Rev. B* **71**, 245319 (2005).

<sup>11</sup>F. J. Giessibl, *Appl. Phys. Lett.* **76**, 1470 (2000).

<sup>12</sup>H. Özgür Özer, M. Atabak, and A. Oral, *Appl. Surf. Sci.* **210**, 12 (2003).

<sup>13</sup>D. Sawada, T. Namikawa, M. Hiragaki, Y. Sugimoto, M. Abe, and S. Morita, *Jpn. J. Appl. Phys.* **47**, 6085 (2008).

<sup>14</sup>Z. Liu, Z. Zhang, and X. Zhu, *Phys. Rev. B* **77**, 035322 (2008); Z. Zhang (personal communication).

<sup>15</sup>M. A. Kulakov, Z. Zhang, A. V. Zotov, B. Bullemer, and I. Eisele, *Appl. Surf. Sci.* **103**, 443 (1996).

<sup>16</sup>T. Komeda and Y. Nishioka, *Appl. Phys. Lett.* **71**, 2277 (1997).

<sup>17</sup>J. Wang, T. A. Arias, and J. D. Joannopoulos, *Phys. Rev. B* **47**, 10497 (1993).

<sup>18</sup>S. R. Schofield and N. J. Curson J. L. O'Brien, M. Simmons, R. G. Clark, N. A. Marks, H. F. Wilson, G. W. Brown, and M. E. Hawley, *Phys. Rev. B* **69**, 085312 (2004).

<sup>19</sup>S. Ihara, S. L. Ho, T. Uda, and M. Hirao, *Phys. Rev. Lett.* **65**, 1909 (1990).

<sup>20</sup>R. J. Hamers and U. K. Köhler, *J. Vac. Sci. Technol. A* **7**, 2854 (1989).

<sup>21</sup>V. A. Ukraintsev, Z. Dohnálek, and J. T. Yates, *Surf. Sci.* **388**, 132 (1997).

<sup>22</sup>G. W. Brown, H. Grube, M. E. Hawley, S. R. Schofield, N. J. Curson, M. Y. Simmons, and R. G. Clark, *J. Appl. Phys.* **92**, 820 (2002).